

# Further performance improvement of $\text{Ba}_{0.5}\text{Sr}_{0.5}\text{Co}_{0.8}\text{Fe}_{0.2}\text{O}_{3-\delta}$ perovskite membranes for air separation

Zhihao Chen<sup>a</sup>, Ran Ran<sup>a</sup>, Zongping Shao<sup>a,\*</sup>, Hai Yu<sup>b</sup>,  
J.C. Diniz da Costa<sup>c</sup>, Shaomin Liu<sup>c,\*</sup>

<sup>a</sup>State Key Laboratory of Materials-oriented Chemical Engineering, Nanjing University of Technology, Nanjing 210009, PR China

<sup>b</sup>Chemical Engineering, The University of Newcastle, Callaghan, NSW 2308, Australia

<sup>c</sup>Films and Inorganic Membrane Laboratory, Division of Chemical Engineering, The University of Queensland, Brisbane, Queensland 4072, Australia

Received 11 July 2008; received in revised form 6 September 2008; accepted 10 February 2009

Available online 11 March 2009

## Abstract

Perovskite  $\text{Ba}_{0.5}\text{Sr}_{0.5}\text{Co}_{0.8}\text{Fe}_{0.2}\text{O}_{3-\delta}$  (BSCF) is a promising mixed conducting ceramic membrane material for air separation. In this work, BSCF powder was synthesized by a modified Pechini sol–gel technique at relatively lower temperature. The  $\text{O}_2$  permeation through a series of BSCF membranes has been tested at different temperatures and various  $\text{O}_2$  partial pressure gradients. Theoretical investigation indicated that bulk diffusion and the  $\text{O}_2$  exchange reactions on membrane surfaces jointly controlled the  $\text{O}_2$  permeation through BSCF membranes with thickness of between 1.1 and 0.75 mm. To further improve the  $\text{O}_2$  fluxes, effective efforts are made on membrane thickness reduction and surface modification by spraying porous BSCF layers on both surfaces. When the membrane thickness was reduced from 0.75 to 0.40 mm, the  $\text{O}_2$  fluxes were increased by 20–60% depending on the operating conditions. The surface modification further improved the  $\text{O}_2$  flux by another 20–40%. The high  $\text{O}_2$  fluxes achieved in this work are quite encouraging with a maximum value reaching  $6.0 \text{ mL min}^{-1} \text{ cm}^{-2}$  at  $900^\circ\text{C}$ .

© 2009 Elsevier Ltd and Techna Group S.r.l. All rights reserved.

**Keywords:** D. Perovskites; Oxygen permeation; Mixed conduction; Surface modification

## 1. Introduction

Global climate change is connected with the rising atmospheric concentration of carbon dioxide from fossil energy use. The production of electricity with no carbon emissions to the atmosphere will become the essential elements of the future power infrastructure transformation. Oxygen production by air separation is of great importance, as most large scale clean coal energy technologies require oxygen as feed gas [1]. For example, if pure oxygen instead of air is used in power plants, the major constituent of the waste gas produced during the combustion process would be  $\text{CO}_2$ , which can be readily and economically captured for geological storage. Current tonnage  $\text{O}_2$  production is based on cryogenic distillation, a 100-year-old technology,

which is expensive and energy intensive because it operates at very low temperature and at elevated pressures. Coupling a cryogenic air separation unit at the front end of a coal gasifier or oxyfuel power plant is unpractical because of its lower power generation efficiencies. Dense mixed ionic and electronic conducting (MIEC) ceramic membranes can continuously deliver 100% pure  $\text{O}_2$  under  $\text{O}_2$  concentration gradient without the requirement of external electrical loadings, offering the potential to tackle these energy penalties and improve the viability of  $\text{CO}_2$  zero emission technology [2–6]. In addition, these MIEC membranes are also of interest as membrane reactors for these high temperature oxidative processes (i.e., gas partial oxidation) to improve the product yield/selectivity beyond what the reaction equilibrium allows [7–9].

From an application point of view, membranes must possess sufficiently high oxygen permeability and good structural stability to withstand real process conditions (i.e., low  $\text{O}_2$  concentration, light hydrocarbon reducing environment, presence of  $\text{CO}_2$  and  $\text{H}_2\text{O}$  vapor). To address these problems, Teraoka et al. developed high oxygen permeation

\* Corresponding authors. Tel.: +86 25 83172256/61 8 92669056; fax: +61 8 92662681.

E-mail addresses: [shaozp@njut.edu.cn](mailto:shaozp@njut.edu.cn) (Z. Shao),  
[shaomin.liu@curtin.edu.au](mailto:shaomin.liu@curtin.edu.au) (S. Liu).

flux membranes from  $\text{SrCo}_{0.8}\text{Fe}_{0.2}\text{O}_{3-\delta}$  perovskite [10]. The high permeation flux was attributed to the high concentration of oxygen vacancy in the lattice due to the total substitution of  $\text{La}^{3+}$  metal ion by  $\text{Sr}^{2+}$  in the A-site of perovskite. Although this material lacks of sufficient chemical and structural stability in practical operation conditions, their breakthrough work inspired the research community to explore new perovskite membranes with improved phase stability and oxygen permeability by optimizing the metal oxide composition in  $\text{ABO}_3$  perovskite structure [4,11–20]. One example is the composition of  $\text{Ba}_{0.5}\text{Sr}_{0.5}\text{Co}_{0.8}\text{Fe}_{0.2}\text{O}_{3-\delta}$  (BSCF), developed from  $\text{SrCo}_{0.8}\text{Fe}_{0.2}\text{O}_{3-\delta}$  by partial substitution of Sr with Ba which possesses a larger ionic radius [4]. It has been found that the BSCF perovskites exhibit not only the highest oxygen permeation flux among these mixed conducting ceramics, but also enhance the phase stability at high temperatures.

Most of previous studies in this area were focused on material synthesis, composition optimization, characterization, stability test and the exploration of oxygen permeation mechanism. In this work, we investigated the oxygen permeation behavior through thicker BSCF plate membranes and provided the proof of concept of the effective ways to further improve the oxygen fluxes by reducing membrane thickness and surface modification. We used the modified Pechini sol–gel technique to prepare the BSCF powder with pure perovskite phase as the starting membrane material. Ethylenediaminetetraacetic acid (EDTA) and citric acid were used jointly as chelating ligands to bind the metal ions and form a stable complexing solution.

## 2. Experimental

### 2.1. BSCF membrane synthesis

$\text{Ba}_{0.5}\text{Sr}_{0.5}\text{Co}_{0.8}\text{Fe}_{0.2}\text{O}_{3-\delta}$  powders investigated in this study were synthesized through a sol–gel process based on an EDTA–citrate complexing method. Appropriate amounts of  $\text{Ba}(\text{NO}_3)_2$ ,  $\text{Sr}(\text{NO}_3)_2$ ,  $\text{Co}(\text{NO}_3)_2 \cdot 6\text{H}_2\text{O}$  and  $\text{Fe}(\text{NO}_3)_3 \cdot 6\text{H}_2\text{O}$  (analytical grades) were used as the raw materials for metal sources. Details of the synthesis procedure have been described elsewhere [21]. The disk-shaped membranes to be used in the oxygen permeation tests were prepared by uni-axial pressing method. Weighed amount of BSCF powder was pressed using a 15 mm stainless steel die under a pressure of 280 MPa. Then the green disks were sintered at 1100 °C for 5 h in air at a heating/cooling rate of 5 °C min<sup>−1</sup>. The sintered membranes have a diameter of 14 mm and were polished to the different thickness ranging from 0.4 to 1.1 mm. The relative density of membranes was measured by the Archimedes method. For surface modification, the porous BSCF layer was spray-deposited on the sintered membrane surface. The BSCF slurry used for spraying was prepared by mixing 5 g BSCF powder, 47 mL isopropanol, 10 mL glycol and 3 mL glycerol. After ball-milling for 1 h in a High Energy Ball Miller, the slurry was spray-deposited on both sides of the membrane surfaces. Then the surface modified membranes were dried at 150 °C for 1 h and then calcined at 1000 °C for 2 h in air with a heating/cooling rate of 2 °C min<sup>−1</sup> to burn out the organic

materials and generate the porous BSCF layer on both sides of the membrane surfaces.

### 2.2. Membrane characterization and oxygen permeation test

The crystal structure of the synthesized powders was characterized by X-ray diffraction (XRD, Bruker D8 Advance) using Cu K $\alpha$  radiation. The morphological and compositional features of the prepared membranes were examined using an environmental scanning electron microscopy (ESEM, QUANTA-2000). The oxygen permeation fluxes of the membranes were measured with a gas chromatography method. Membranes were sealed with a silver paste onto the quartz support tubes. The sidewall of the membrane disks was also covered with the sealant to avoid leakage and radial contribution to the oxygen flux. Ambient air was used as the feed gas (oxygen rich-side atmosphere) and helium with various flow rates as the sweep gas (oxygen lean side atmosphere). A gas chromatograph (CP 3800, Varian) equipped with a 5 Å molecular sieve capillary column was used to in-situ analyze the composition of the outlet gas.

## 3. Results and discussion

### 3.1. BSCF membrane synthesis

With the condensing process by water evaporation, a deep-purple transparent gel was obtained. Because no precipitation occurred over the entire condensation process, the compositional homogeneity of metal ion distribution on the atomic level in the aqueous solution could be well maintained in the resulting gels. This gel was transformed into the BSCF precursor powder by heating the gel at 250 °C for 24 h. BSCF perovskite with desired structure was obtained by heating the precursor powder at high temperatures. The crystalline phase development as a function of calcining temperature is depicted by the XRD patterns plotted in Fig. 1. The sample calcined at the temperature of 500 °C is the mixture of metal oxides, carbonates and other unidentified intermediate phases. At 800 °C or above, the XRD spectra exhibit the patterns having seven strong diffraction peaks with respective  $2\theta$  angles and lattice planes of 22.28 {1 0 0}, 31.72 {1 1 0}, 39.24 {1 1 1}, 45.52 {2 0 0}, 56.60 {2 1 1}, 66.36 {2 2 0}, and 75.72 {3 1 0}, which have previously been related to the cubic perovskite phase of BSCF as shown in Fig. 1(b–d) [4]. In this work, the BSCF powder used as the starting membrane material was prepared at 900 °C. By contrast, a sintering temperature of 1150 °C and a processing time of 10 h are required by the conventional solid-state reaction method for the same purpose. The present research shows a substantial decrease of the processing time and temperature required for the formation of the desired single-phase perovskite structure. Using the prepared perovskite powder as the starting membrane material, most of the sintered membranes are gas tight and have the relative density larger than 95% tested by the Archimedes method.

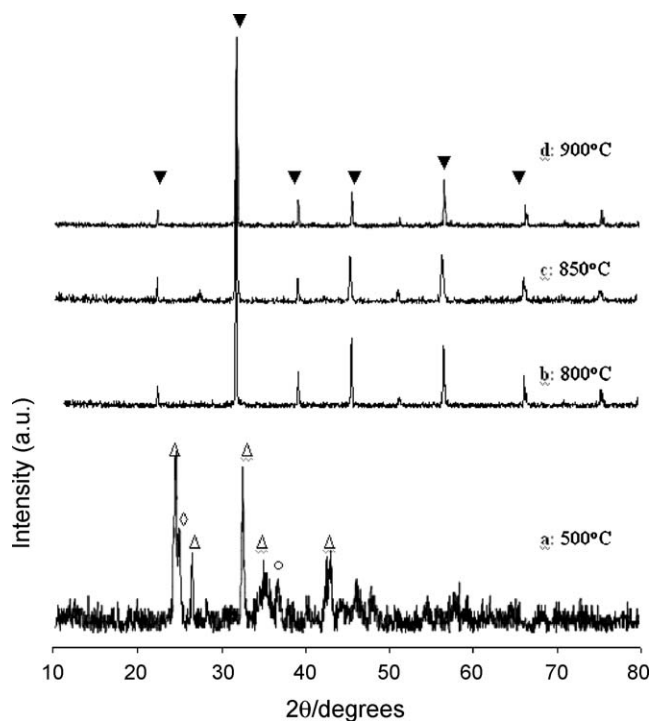


Fig. 1. XRD patterns of the powders by calcination of the BSCF precursor powder at different temperatures (▼, ○, ◇, and △ stand for the peaks of perovskite,  $\text{Co}_3\text{O}_4$ ,  $\text{SrCO}_3$ , and some unknown phases, respectively).

### 3.2. $\text{O}_2$ permeation through BSCF plate membranes with thickness of 1.1 and 0.75 mm

$\text{O}_2$  permeation through two BSCF membranes with thickness of 1.1 (Membr-I) and 0.75 mm (Membr-II) was tested by introducing air flow as feed gas and He as sweep gas separately in the two sides of the membranes. At high temperatures, oxygen will permeate from the air side to the permeate side having sweep gas because of the oxygen concentration gradient across the membrane. At the He sweep gas flow rate of  $100 \text{ mL min}^{-1}$ , the effect of temperature on  $\text{O}_2$  permeation flux was investigated from 550 to  $900^\circ\text{C}$ . At temperatures below  $600^\circ\text{C}$ , the  $\text{O}_2$  fluxes were very small and appreciable high oxygen permeation can only occur at temperatures above  $700^\circ\text{C}$ . Fig. 2a shows that the operating temperature dependency on  $\text{O}_2$  fluxes through two samples is in almost linear trend. The improvement of  $\text{O}_2$  fluxes with temperature is due to the enhancement of oxygen diffusion and surface reaction rate at high temperatures. For example, the oxygen fluxes through Membrane-I was increased by  $1.41 \text{ mL min}^{-1} \text{ cm}^{-2}$  from  $1.65$  ( $750^\circ\text{C}$ ) to  $3.06 \text{ mL min}^{-1} \text{ cm}^{-2}$  ( $900^\circ\text{C}$ ) and through Membrane-II by  $1.54 \text{ mL min}^{-1} \text{ cm}^{-2}$  from  $1.93$  ( $750^\circ\text{C}$ ) to  $3.47 \text{ mL min}^{-1} \text{ cm}^{-2}$  ( $900^\circ\text{C}$ ). Fig. 2b shows Arrhenius plots of oxygen permeation through the two membranes. Activation energies for oxygen transport through Membranes-I and -II under the conditions of Fig. 2a are  $43.5$  and  $41.2 \text{ kJ/mol}$ , respectively.

$\text{O}_2$  flux through dense mixed ionic and electronic perovskite membranes are essentially controlled by two factors: the rate of

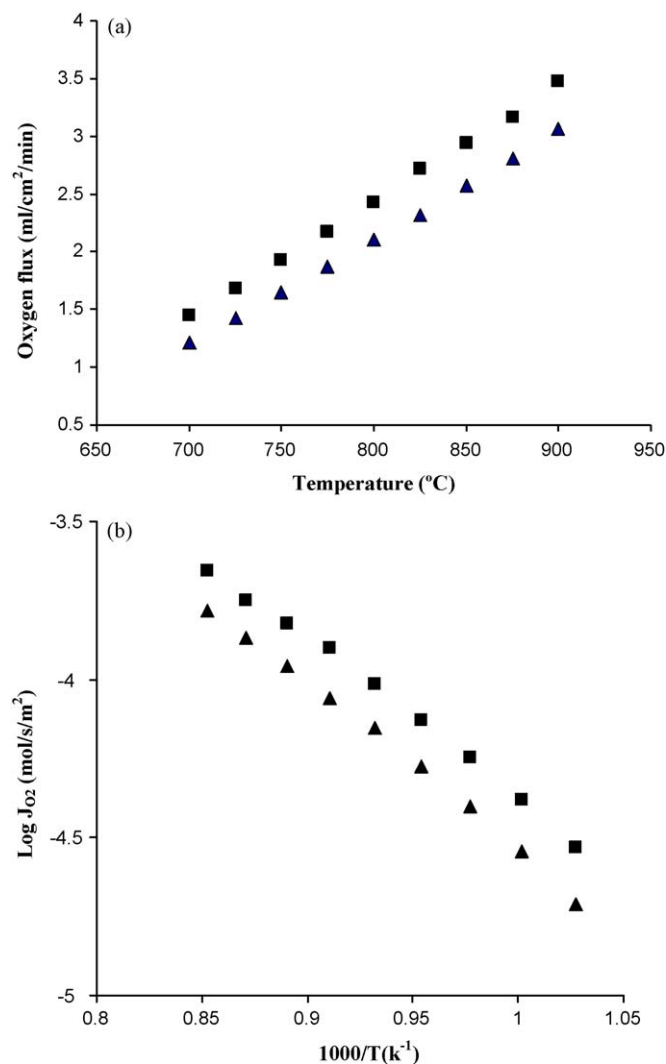


Fig. 2. Effect of operating temperature on the oxygen fluxes through membranes (a) and Arrhenius plot (b) (▼: Membr-I with thickness 1.1 mm; ■: Membr-II with thickness 0.75 mm).

oxygen diffusion through the bulk of membrane and the two surface reactions for oxygen exchange. Under the bulk diffusion controlling step, the oxygen permeation flux through a membrane exposed to a chemical potential gradient can be generally described by Wagner's equation,

$$J_{\text{O}_2} = -\frac{RT}{4^2 F^2 L} \int_{\ln P'_{\text{O}_2}}^{\ln P''_{\text{O}_2}} \frac{\sigma_{\text{ion}} \sigma_{\text{el}}}{\sigma_{\text{ion}} + \sigma_{\text{el}}} d[\ln P_{\text{O}_2}] \quad (1)$$

where  $\sigma_{\text{ion}}$ ,  $\sigma_{\text{el}}$ ,  $F$ ,  $L$ ,  $P'_{\text{O}_2}$  and  $P''_{\text{O}_2}$  stand for the oxygen ionic conductivity, electronic conductivity, the Faraday constant, the membrane thickness, the oxygen rich-side and oxygen lean-side partial pressure, respectively. Eq. (1) illustrates that the permeation flux is also influenced by the material property (oxygen ionic and electronic conductivity). In our previous work, the maximum electronic conductivities of BSCF under air atmosphere can reach around  $40 \text{ S cm}^{-1}$ , while the oxygen ionic conductivity of BSCF is only about  $1.4 \text{ S cm}^{-1}$  at  $900^\circ\text{C}$  [22,23]. With the overwhelming electronic conductivity over

oxygen ionic one in BSCF, Eq. (1) can be simplified as

$$J_{O_2} = -\frac{RT}{4^2 F^2 L} \int_{\ln P'_{O_2}}^{\ln P''_{O_2}} \sigma_{ion} d[\ln P_{O_2}] \quad (2)$$

The relationship of  $\sigma_{ion}$  and oxygen partial pressure can be expressed by the empirical equation of

$$\sigma_{ion} = \sigma_{ion}^O P_{O_2}^n \quad (3)$$

Combining (2) and (3) gives

$$J_{O_2} = \frac{\beta}{L} [P''_{O_2} n - P'_{O_2} n] = a [P''_{O_2} n - P'_{O_2} n] \quad (4)$$

Where

$$\beta = -\frac{\sigma_{ion}^O RT}{4^2 F^2 n}$$

On the other hand, according to the theoretical work by Xu and Thomson [24], when the membrane thickness is far less than the critical thickness, the  $O_2$  permeation is mainly determined by the surface-exchange kinetics. The following equation can be derived for  $O_2$  permeation fluxes:

$$J_{O_2} = \frac{k_r (P'_{O_2} 0.5 - P''_{O_2} 0.5)}{(P'_{O_2} 0.5 + P''_{O_2} 0.5)} \quad (5)$$

Where  $k_r$  is the surface exchange rate constant.

From the value of  $n$  in Eq. (4), the rate limiting step of the  $O_2$  permeation can be roughly identified. For  $n < 0$ , bulk diffusion of the oxygen ion is the rate-limiting step, while for  $n \geq 0.5$ , the reaction of molecular oxygen with the membrane surfaces is the rate-controlling step. For  $0 < n < 0.5$ , the oxygen permeation is jointly controlled by both surface reactions and bulk diffusion.

Fig. 3 displays the effects of oxygen partial pressure in the permeate side on  $O_2$  permeation at 900 °C. As can be seen, decrease in  $O_2$  partial pressure by increasing sweep gas rates resulted in higher oxygen fluxes. For instance, increasing the He flow rate from 20 to 260 mL min<sup>-1</sup> lowered the  $O_2$  partial pressure from 0.031 to 0.0058 atm and improved the  $O_2$  fluxes through Membr-I from 2.33 to 3.52 mL min<sup>-1</sup> cm<sup>-2</sup>. Eq. (4) can be used to describe the oxygen permeation behavior through two thicker BSCF membranes at the investigated temperature range. For comparison purpose, two typical theoretical results from Eq. (4) by regression analysis based on the Least Squares were also presented as the solid lines in Fig. 3. The modeling results fit very well with the experimental data for two membrane samples examined. The observation of positive values of 0.33 and 0.12 indicates that both processes of bulk diffusion and surface reactions jointly influenced the  $O_2$  permeation process. In this case, to further improve the  $O_2$  fluxes through the BSCF membranes, efforts should be placed on the membrane thickness reduction and surface modification.

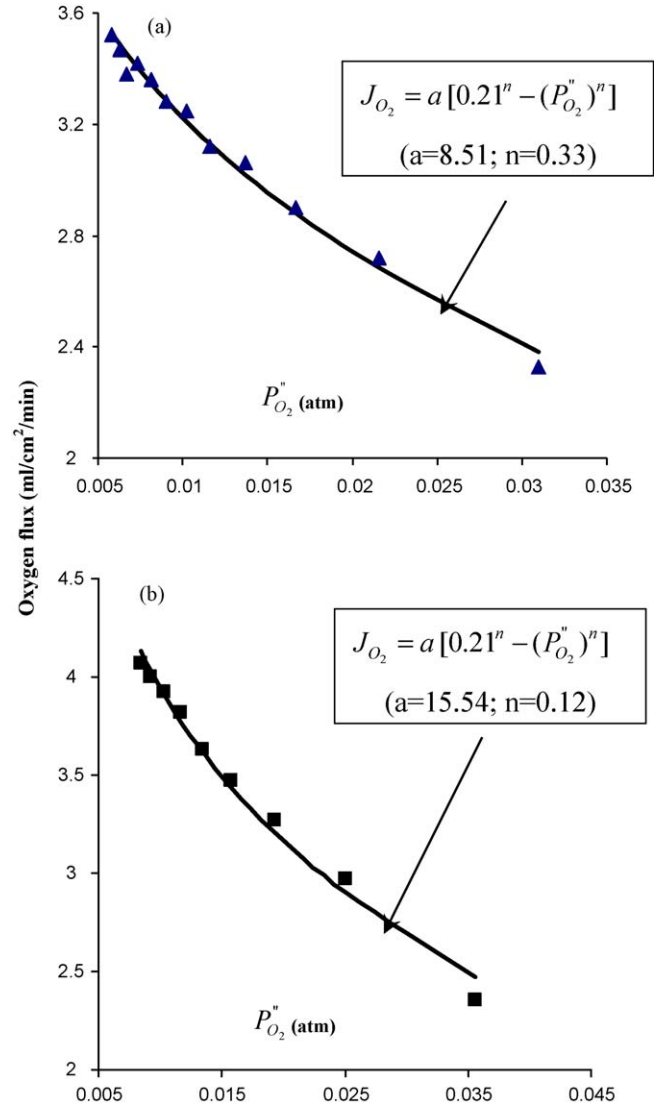


Fig. 3. Experimental and modeling results of the effect of oxygen partial pressure in the permeate side on the oxygen fluxes through two membranes at 900 °C ((a) Membr-I (▲: experimental); (b) Membr-II (■: experimental)).

### 3.3. Oxygen permeation through BSCF membrane with reduced thickness (0.4 mm) and surface modification

Membr-III with thickness of 0.4 mm was prepared with similar surface morphologies as these of Membr-I and II. Membr-III exhibited much improved performance in terms of permeation rate. Fig. 4 shows the  $P''_{O_2}$  dependence of oxygen permeation fluxes. Compared to Membr-II, Membr-III further improved the oxygen flux by 20 to 60% depending on the operating temperatures. For example, at 800 °C and He gas rate of 100 mL min<sup>-1</sup>, the oxygen fluxes through Membr-II with thickness of 0.75 mm was 2.43 mL min<sup>-1</sup> cm<sup>-2</sup>; at similar conditions, the  $O_2$  flux through Membr-III were improved by 38% and reached 3.35 mL min<sup>-1</sup> cm<sup>-2</sup>. To give another example as shown in Fig. 4b, at 900 °C and similar  $O_2$  partial pressure in the permeate side ( $P''_{O_2}$ ) of 0.02 atm, Membr-III gave  $O_2$  flux of 5.1 mL min<sup>-1</sup> cm<sup>-2</sup> in contrast to the lower value of 3.2 mL min<sup>-1</sup> cm<sup>-2</sup> by Membr-II. The better performance



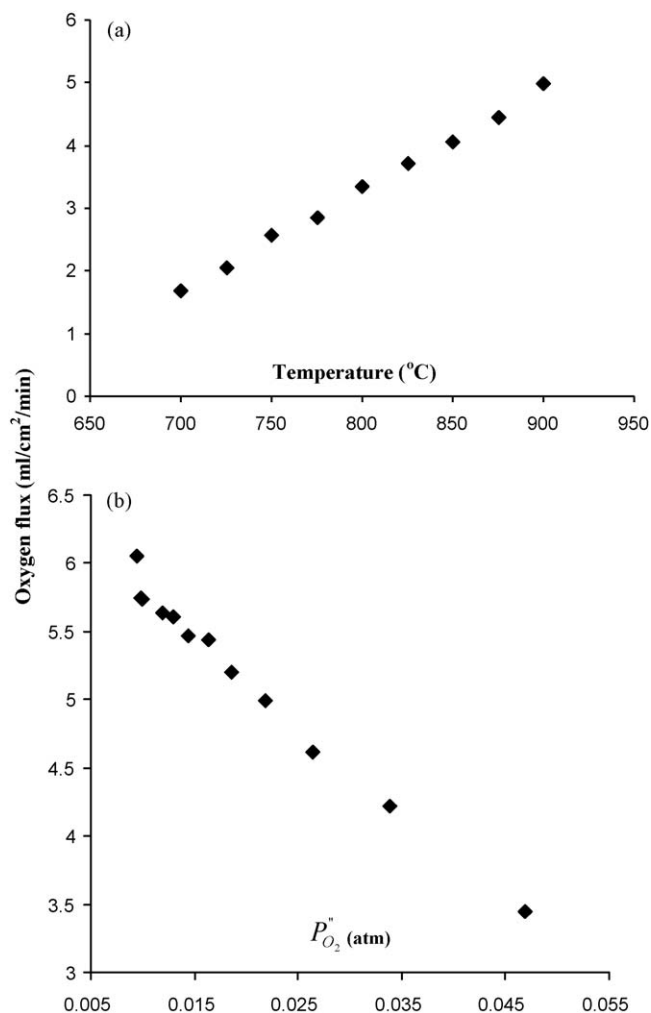


Fig. 4. Effect of operating temperature (a) and oxygen partial pressure in the permeate side at 900 °C (b) on the oxygen fluxes through Membr-III (Membr-III with thickness 0.4 mm).

of Membr-III is closely related to its thinner thickness which provides less mass transport resistance for oxygen ion diffusion. The thickness of plate membrane is often much larger than the critical thickness at which the oxygen permeation is equally determined by the surface-exchange kinetics and bulk-diffusion. In this case, to maximize the oxygen flux, BSCF membranes should be prepared as thin as possible. However, under our laboratory conditions, BSCF plate with 0.4 mm thickness was the thinnest membrane which can be prepared by pressing method. For the fabrication of ultra-thin BSCF plate membranes, coating technology has to be employed.

As discussed above, when the BSCF membrane thickness is less than 1.1 mm, the surface reactions between molecular oxygen, lattice oxygen, oxygen vacancies and electron-holes already play an import role in the determination of oxygen permeation rate. Therefore, membrane surface modification to promote the reaction kinetics will also be effective to increase the oxygen permeation rate. Surface modification can be achieved by coating a more porous layer with higher surface area or by deposition of catalyst of superior O<sub>2</sub> exchanging properties. In this work, Membr-III was further coated with

porous layer of the same BSCF material. This avoids the unfavorable reaction between the two different materials employed or the peeling off of the porous layer due to the mismatch of different thermal expansion. Fig. 5 shows the SEM pictures of Membr-III and its modified BSCF membrane (Sample IV) surface and cross-sectional views. Fig. 5a shows the polished surface of Membr-III is quite smooth and the grain boundary of BSCF particles cannot be distinguished. It should be noted that the membranes are not 100% densified and there are still many isolated pores along the cross section area; however, there is no connected porosity across the membranes. After spray coating, the porous BSCF layer with thickness of 15 μm, consisting of agglomerated 3 μm-sized particles, integrates well to the original membrane surface as shown in Fig. 5b (marked with blue rectangles).

The effect of surface modification on oxygen permeation was further investigated as depicted in Fig. 6. Compared to the original membrane (Membr-III) with similar densified thickness of 0.4 mm, the performance of the membrane after the deposition of porous layer (Membr-IV) in oxygen permeation was improved by 20 to 40% with relatively larger improvement at lower temperatures. For instance, at 700 and 900 °C, the O<sub>2</sub> permeation fluxes were increased from 1.68 to 2.35 and 5.0 to 6.0 mL min<sup>-1</sup> cm<sup>-2</sup>, respectively. Such significant improvement on oxygen permeation flux of BSCF is due to the surface modification with porous layer which enlarges the surface area for oxygen exchange reaction.

So far, a series of perovskite oxides with a general stoichiometric formula of A<sub>y</sub>A'<sub>(1-y)</sub>B<sub>x</sub>B'<sub>(1-x)</sub>O<sub>(3-α)</sub> have been reported to possess appreciably high oxygen permeation rate [4,10–20]. The A, A', B and B' elements can be selected from La, Sr, Ba, Ca, Zr, Mg, Al, Ti, Cr, Mn, Fe, Co, Ni, Cu, Ga, Zr, or Z and x/y is ranged from 0–1. Among the mixed conducting plate membranes tested in the literature, the O<sub>2</sub> fluxes achieved in the present work are the highest. For BSCF hollow fibre membranes with a thickness of 0.25 mm, Liu and Gavallas reported a maximum oxygen flux of 2.8 mL min<sup>-1</sup> cm<sup>-2</sup> at 900 °C [25]. The fluxes measured in the current study was up to 6.0 mL min<sup>-1</sup> cm<sup>-2</sup> with membrane thickness of 0.4 mm and surface modification. The contamination by sulfur during the preparation is one of possible reasons for the lower permeation rates of these BSCF hollow fibres [25].

It has been suggested that when the permeation flux through a mixed conducting ceramic membrane is larger than 10 mL min<sup>-1</sup> cm<sup>-2</sup> [STP] (7.44 × 10<sup>-6</sup> mol cm<sup>-2</sup> s<sup>-1</sup>) [26,27], the membrane can be considered for large-scale application to replace the traditional cryogenic method which is energy-intensive and cannot be economically applied for clean energy deliveries. According to the theoretical prediction in Fig. 3b, when the O<sub>2</sub> pressure in the permeate side is less than 10<sup>-5</sup> atm (i.e., by applying vacuum), the O<sub>2</sub> flux through Membr-III with 0.4 mm-thickness will reach 9.0 mL min<sup>-1</sup> cm<sup>-2</sup>. Based on the result of surface modification, the O<sub>2</sub> flux through Membr-IV operated at this condition can be up to 11 mL min<sup>-1</sup> cm<sup>-2</sup> approaching the target of commercial interest.

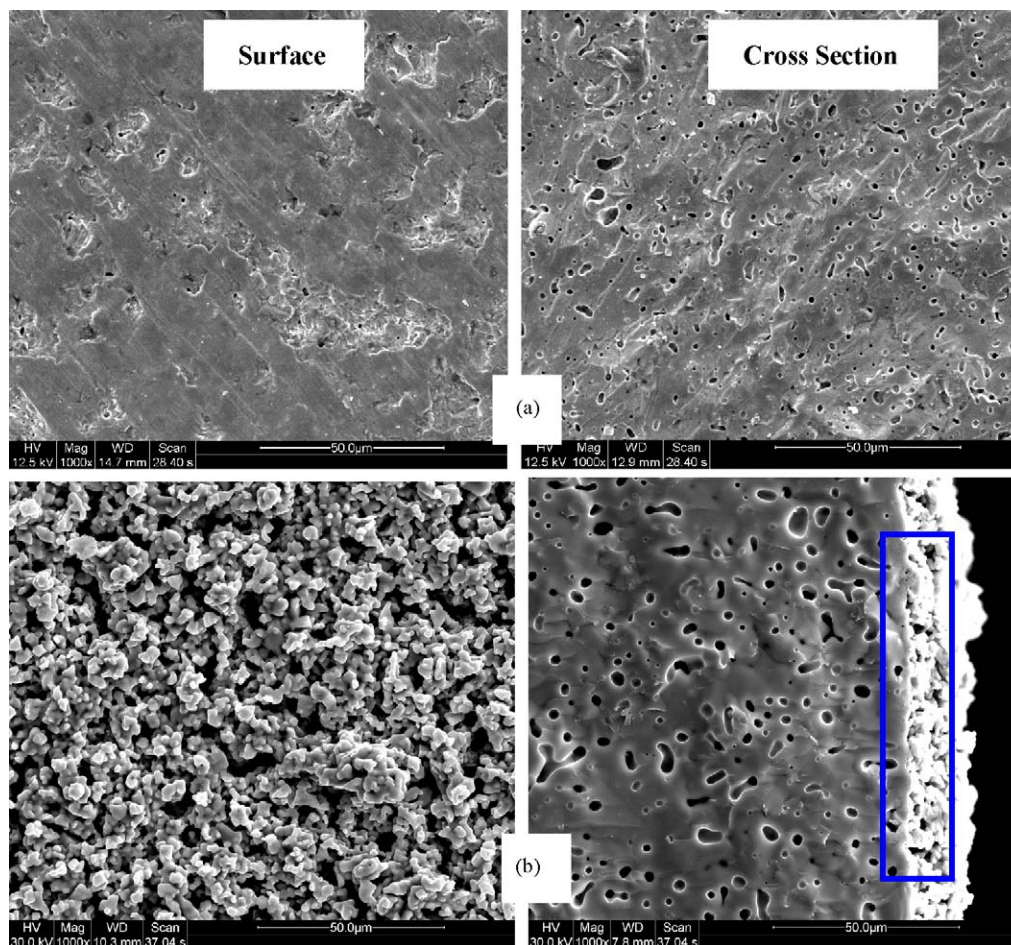


Fig. 5. SEM micrographs of the BSCF membranes ((a) Membr-III with thickness of 0.4 mm; (b) Membr-IV after surface modification of Membr-III by spray coating).

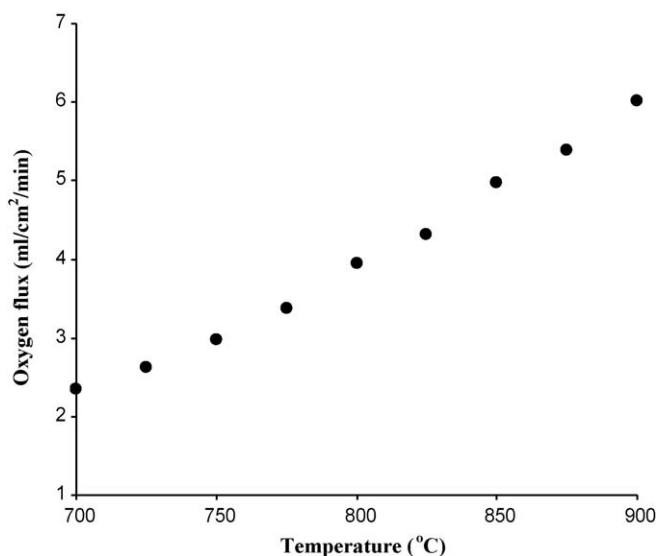


Fig. 6. Effect of operating temperature on the oxygen fluxes through Membr-IV.

#### 4. Conclusion

High quality BSCF powder to be used as membrane material with pure perovskite phase was prepared via a modified Pechini

sol-gel technique.  $O_2$  permeation was experimentally and theoretically investigated based on a series of BSCF plate membranes. Theoretical analysis implied that oxygen permeation was jointly controlled by surface modification and bulk diffusion when the BSCF membrane thickness was less than or equal to 1.1 mm. Reducing membrane thickness to 0.45 mm improved the fluxes by 20–60% compared to the membrane of 0.75 mm thickness. Membrane modification was achieved by spraying a porous BSCF layer on both surfaces with thickness of 15  $\mu$ .  $O_2$  fluxes through the surface modified membrane were further improved by 20–40% depending on the operating conditions. The maximum flux achieved in this work reached  $6.0 \text{ mL min}^{-1} \text{ cm}^{-2}$  at  $900^\circ\text{C}$ , which is the highest value among all the plate membrane reported in the literature. The encouraging permeation value together with the good operational stability reported in previous work makes the  $\text{Ba}_{0.5}\text{Sr}_{0.5}\text{Co}_{0.8}\text{Fe}_{0.2}\text{O}_{3-\delta}$  material interesting as a mixed conducting ceramic membrane for large-scale applications.

#### Acknowledgement

This work was supported by the National Natural Science Foundation of China under contracts Numbers of 20646002 and 20676061. Dr. Yu is particularly grateful to the University of

Newcastle, Australia, for providing the research fund under the Independent Investigator Research Scheme for 2008. Dr. Liu acknowledges the ARC fellowship provided by the Australian Research Council.

## References

- [1] B.J. Jody, E.J. Daniels, A.M. Wolsky, Integrating  $O_2$  production with power systems to capture  $CO_2$ , *Energy Convers. Manage.* 38 (1997) S135.
- [2] S.P.S. Badwal, F.T. Ciacchi, Ceramic membrane technologies for oxygen separation, *Adv. Mater.* 13 (2001) 993.
- [3] P.N. Dyer, R.E. Richards, S.L. Russek, D.M. Taylor, Ion transport membrane technology for oxygen separation and syngas production, *Solid State Ionics* 134 (2000) 21.
- [4] Z. Shao, W. Yang, Y. Cong, H. Dong, J. Tong, G. Xiong, Investigation of the permeation behavior and stability of a  $Ba_{0.5}Sr_{0.5}Co_{0.8}Fe_{0.2}O_{3-\alpha}$  oxygen membrane, *J. Membr. Sci.* 172 (2000) 177.
- [5] W. Jin, S. Li, P. Huang, N. Xu, J. Shi, Preparation of an asymmetric perovskite-type membrane and its oxygen permeability, *J. Membr. Sci.* 185 (2001) 237.
- [6] Y. Liu, X. Tan, K. Li, Mixed conducting ceramics for catalytic membrane processing, *Catal. Rev.* 48 (2006) 145.
- [7] H.J.M. Bouwmeester, Dense ceramic membranes for methane conversion, *Catal. Today* 82 (2003) 141.
- [8] Z. Shao, H. Dong, G. Xiong, Y. Gong, W.S. Yang, Performance of a mixed-conducting ceramic membrane reactor with high oxygen permeability for methane conversion, *J. Membr. Sci.* 183 (2001) 181.
- [9] J.E. ten Elshof, H.J.M. Bouwmeester, H. Verweij, Oxidative coupling of methane in a mixed-conducting perovskite membrane reactor, *Appl. Catal. A: Gen.* 130 (1995) 195.
- [10] Y. Teraoka, H. Zhang, S. Furukawa, N. Yamazoe, Oxygen permeation through perovskite-type oxides, *Chem. Lett.* 11 (1985) 1743.
- [11] J.H. Tong, W.S. Yang, B.C. Zhu, Investigation of Ideal Zirconium-doped Perovskite-type Ceramic Membrane Materials for Oxygen Separation, *J. Membr. Sci.* 203 (2002) 175–189.
- [12] F.M. Figueiredo, V.V. Kharton, A.P. Viskup, J.R. Frade, Surface Enhanced Oxygen Permeation in  $CaTi_{1-x}Fe_xO_{3-\alpha}$  Ceramic Membranes, *J. Membr. Sci.* 236 (2004) 73–80.
- [13] H. Wang, C. Tablet, A. Feldhoff, J. Caro, A Cobalt-free oxygen-permeable membrane based on the perovskite-type oxide  $Ba_{0.5}Sr_{0.5}Zn_{0.2}Fe_{0.8}O_{3-\alpha}$ , *Adv. Mater.* 17 (2005) 1785–1789.
- [14] W.S. Yang, H. Wang, X.F. Zhu, L.W. Lin, Development and Application of Oxygen Permeable Membrane in Selective Oxidation of Light Alkanes, *Top. Catal.* 35 (2005) 155–167.
- [15] A.A. Yaremchenko, V.V. Kharton, A.P. Viskup, E.N. Naumovich, V.N. Tikhonovich, N.M. Lapchuk, Mixed electronic and ionic conductivity of  $LaCo(M)O_3$  ( $M = Ga, Cr, Fe$  or  $Ni$ ), *Solid State Ionics* 120 (1999) 65.
- [16] S. Diethelm, J. Van Herle, P.H. Middleton, D. Favrat, Oxygen permeation and stability of  $La_{0.4}Ca_{0.6}Fe_{1-x}Co_xO_{3-\delta}$  ( $x = 0, 0.25, 0.5$ ) membranes, *J. Power Sources* 118 (2003) 270.
- [17] S. Diethelm, J. Van Herle, Oxygen transport through dense  $La_{0.6}Sr_{0.4}Fe_{0.8}Co_{0.2}O_{3-\delta}$  perovskite-type permeation membranes, *J. Eur. Ceram. Soc.* 24 (2004) 1319.
- [18] J.M. Kim, G.J. Hwang, S.H. Lee, C.S. Park, J.W. Kim, Y.H. Kim, Properties of oxygen permeation and partial oxidation of membrane in  $La_{0.6}Sr_{0.4}CoO_{3-\delta}$  (LSC)– $La_{0.7}Sr_{0.3}Ga_{0.6}Fe_{0.4}O_{3-\delta}$  (LSGF) membranes, *J. Membr. Sci.* 250 (2005) 11.
- [19] X.F. Zhu, H.H. Wang, W.S. Yang, Novel cobalt-free oxygen permeable membrane, *Chem. Commun.* 9 (2004) 1130.
- [20] T. Ishihara, T. Yamada, H. Arikawa, H. Nishiguchi, Y. Takita, Mixed electronic-oxide ionic conductivity and oxygen permeating property of Fe-, Co- or Ni-doped  $LaGaO_3$  perovskite oxide, *Solid State Ionics* 135 (2000) 631.
- [21] W. Zhou, Z.P. Shao, W.Q. Jin, Synthesis of nanocrystalline conducting composite oxides based on a non-ion selective combined complexing process for functional applications, *J. Alloy Compd.* 426 (2006) 368.
- [22] Z.H. Chen, R. Ran, W. Zhou, Z.P. Shao, S.M. Liu, Assessment of  $Ba_{0.5}Sr_{0.5}Co_{1-y}Fe_yO_{3-\delta}$  ( $y = 0.0$ – $1.0$ ) for prospective application as cathode for IT-SOFCs or oxygen permeating membrane, *Electrochimica Acta* 52 (2007) 7343.
- [23] Z.H. Chen, Z.P. Shao, R. Ran, W. Zhou, P.Y. Zeng, S.M. Liu, A dense oxygen separation membrane with a layered morphologic structure, *J. Membr. Sci.* 300 (2007) 182.
- [24] S.J. Xu, W.J. Thomson, Oxygen permeation rates through ion-conducting perovskite membranes, *Chem. Eng. Sci.* 54 (1999) 3839.
- [25] S. Liu, G.R. Gavalas, Preparation of oxygen ion conducting ceramic hollow fiber membranes, *Ind. Eng. Chem. Res.* 44 (2005) 7633.
- [26] R. Bredesen, J. Sogge, in: Seminar on the Ecological Applications of Innovative Membrane Technology in the Chemical Industry, Chem/Sem. 21/R.12, 1996, Cetaro, Calabria, Italy.
- [27] P.V. Hendriksen, P.H. Larsen, M. Mogensen, F.W. Poulsen, K. Wiik, Prospects and problems of dense oxygen permeable membranes, *Catal. Today* 56 (2000) 283.